Concrete in a severe freezing environment: a meteorological characterization

Laurent Izoret, Sara Al Haj Sleiman, Nadare Matoiri-Chaibati, Frédéric Grondin

CONCRETE IN SEVERE FREEZING ENVIRONMENT

A meteorological characterization

Laurent IZORET[a], Sara AL HAJ SLEIMAN[a,b]

Nadare MATOIRI-CHAIBATI[a,c], Frédéric GRONDIN[b]

[a] *ATILH, 7, place de la défense 92974 Paris-la-Défense Cedex. France*

l.izoret@atilh.fr

[b] *Institut de Recherche en Génie Civil et Mécanique (GeM), UMR 6183, Centrale Nantes – Université de Nantes – CNRS, 1 rue de la Noë, 44321 Nantes, France*

sara.al-haj-sleiman@ec-nantes.fr; frederic.grondin@ec-nantes.fr

[c] *Laboratoire Angevin de Recherche en Ingénierie des Systèmes, LARIS, EA 7315, UNIV Angers, SFR MathSTIC, 62 Avenue Notre-Dame-du-Lac, 49000 Angers, France*

matoirich@gmail.com

Abstract

Comparing the different test methods for concrete resistance to scaling and the crucial lack of correlation between the laboratory test results and the field results, their representativeness can be questioned. Many researchers tried to clarify most of the mechanisms involved in the damages due to scaling, as well as thermal parameters influencing damage intensity. However, it is remarkable that the prediction of the degradation in relation to mix design characteristics remains unreliable and seems to be disconnected from the performance on site. Moreover, the interpretation of the test results also remains difficult, appearing in contradiction with the first order parameters e.g. minimum freezing temperature or freezing rate. These considerations led us to undertake some measurements campaigns in order to characterize the concrete's temperature response to severe freezing environment, this environment being itself fully characterized by a set of relevant meteorological parameters measured on field site, very closed to the samples.

In this paper, we present the results of three years of meteorological measurements (2013-2016) from two concrete blocks placed in a complete meteorological station located in a severe freezing environment. The temperature measurements were taken on one hand from an XF4 concrete block equipped with thermocouples placed at 2 and 8.5 cm deep and on the other hand from the temperature of the air mass coming from a Stevenson shelter with double shelf in opposite orientation, both compared to the laboratory thermal cycle according to CEN/TC12390-9 (Slab test). If this latter is giving a very symmetrical and periodic temperature signal, the first one is rather characterized by a strong asymmetry and irregularity in profile and full amplitude. We show that the natural conditions are very far from the laboratory conditions in terms of full amplitude, freezing rates and frequency of freezing-thawing cycles. In addition, we show that these field conditions are representative of severe freezing environment according to EN 206 standard, in the French Alps as well as in the Nordic conditions which can be found in Norway, Sweden and Finland.

Keywords: thermal cycles, freeze and thaw, concrete, severe frost zone, statistical analysis, numerical modeling.

1. Introduction

Durability of concrete is a multi-criteria property which has to be assessed to ensure sustainable constructions (protection of people and goods) with optimised costs of maintenance. Among the several parameters of durability, freeze-thaw resistance can be one of the major factors that affect concrete structure; eventually in combination with other parameters e.g. carbonation and chlorine ingress from de-icing salts (NaCl, $CaCl_2$).

Assessment of the durability of concrete in winter environment is made through a set of freeze-thaw tests making a clear distinction between the damages caused by the frost action affecting the concrete structure: internal cracking (structural) and external damages due to the combination of freeze-thaw cycles and de-icing salts (scaling) affecting the outer surface of concrete.

If the test methods for internal damages are reliable with good correlations between mix design parameters and curing effect such as air voids distribution (e.g. Powers in **[1],** Pigeon et al. in **[2]** and Bager and Sellevold in **[3])** and performance in terms of resistance to freeze and thaw (e.g. **[4]**, **[5]**) , the test methods assessing scaling effect remain with a poor reliability due to poor fidelity data (**[6]–[8])**, avoiding their recognition as standardized test methods but as a technical specifications [9]**.** The three main methods, described in CEN/TS 12390-9 are based on a multitude of thermal cycles whose only common characteristics is the full amplitude of temperature (peak to peak) of 40°C [+20°C/-20°C], except for the German Cube with a full amplitude of 35°C [+20/-15°C] over a period of time of 24h, except for CDF Test, over 12h. These conditions induce variable freezing rates, ranging from 1.5°C/h (German cube) to 10°C/h (CDF Test: Capillary suction, De-icing agent and Freeze-thaw-test). In addition, there are different practical exposures to saline solution: gravimetric percolation (Scandinavian slab test), full immersion (German cube test) or capillary suction (German CDF test).
As a result, the quantitative values of scaling from the test results are difficult to compare with different limit values for assessment: CDF test 1.5 kg/m^2 versus Slab test at 0.6 kg/m^2, associated with poor repeatability and reproducibility characteristics.

As these test methods are based on +20°C/-20°C amplitude of the thermal cycle, they are hence supposed to take into account all the thermal constraints affecting the intensity of degradation **[9–12]** and to be representative of cold climate e.g. severe freezing environment. However, the temperature extremum are defined by some practical considerations: +20°C is required to get full thawing of the samples and -20°C is defined by the range of stability of calorific capacity of water **[14]**, **[15]**. This environment should correspond to the winter conditions in Nordic countries or mountain environment in western and central Europe i.e. Alpine Arch in Switzerland, Italy, Germany and France. For this last country, according to EN 206/CN, a severe freezing environment is defined by more than 10 days per year with a minimum temperature equal or below -10°C. This definition was established on the basis of measurements over a period of 30 years from 108 meteorological stations and did not take into consideration the sun exposure and micro- climatic effects.

Numerous field evidences show that degradations due to freeze-thaw scaling occur under much milder local climate conditions compared to the laboratory conventional conditions. Considering the very high scattering of the all-test methods, the representativeness

of the temperature profile as well as the suitability of the whole test methods can be reasonably questioned, including the applicability of such methods for milder climates. When questioning the test method representativeness, the methodological approach is to correlate the laboratory test results with the deterioration of concrete samples with the same concrete mix design placed in a natural environment. The first large scale experiment of this type was done under BRITE Project in 1992 **[16].** The study suffers from a weak characterization of natural environment in contradiction to well characterized laboratory conditions.

A first experiment was done during the winter 1991-92 by placing a concrete block equipped with thermocouples at the Météo-France Snow Study Centre (Centre d'Etude de la Neige) located in the Chartreuse massif near Grenoble, at an altitude of 1,326 m. The temperature profiles of concrete were very dissymmetrical showing positive peaks of temperature up to 15°C and negative peaks down to -6°C. The corresponding rates were registered at 2.5°C/h as cooling rate and freezing rate ranging from 0.4 to 0.75°C/h. Due to a lack of characterisation of the natural environment, the interpretation of the recorded temperature data was limited and did not lead to relevant conclusions by Izoret **[17]**, confirming the above statement.

Based on these observations, it appeared that the assessment of the representativeness of a durability test method on freeze-thaw should start by the measurement of the concrete response to its natural environment with regards to temperature. This natural environment must be characterized as largely as possible in order to fully interpret the temperature signal in terms of first and second order meteorological parameters influencing the temperature of concrete. In these conditions, the relevant data will be used for thermal modeling of concrete.

Subsequently, a set of two concrete blocks equipped with thermocouples were exposed in natural conditions at the Mount Aigoual meteorological station located in a severe freezing environment. The initial aim of this study was to compare concrete's behaviours of a traditional mix design XF4 with air- entrained, with a Ultra High Performance Fiber Reinforced concrete (UHPFRC) without air entrained. In this paper we only report the temperature evolution of XF4 concrete placed in its natural winter environment. These two concrete mix designs were used to cast the blocks, one corresponding to a XF4 mix design with air entrained and one corresponding to an Ultra High Performance Fiber reinforced concrete (UHPFRC). After having established the relevant correlations between meteorological parameters and the concrete response, the selected data were used for thermal modeling of hardened concrete in order to recalculate the time resolved temperature signal. A good fit between measured and calculated temperature profiles implies a full understanding of the relevant parameters determining the concrete temperature in its winter environment. In addition, the temperature fluctuations were compared to the conventional freeze-thaw cycle according to CEN/TS12390-9 (slab-test).

2. Field experimentation at Mount Aigoual meteorological station

2.1 Chosen location and its representativeness

The meteorological station of Mount Aigoual (44° 07’ 15’’ N / 3° 34’ 53’’ E), located at the southern boundary of the Cevennes mountain in the southern part of France is chosen for the experimental program for several reasons; i) it is a full meteorological station dedicated to observations, measurements and experiments, ii) it is an official Météo-France test centre ensuring certified measurements data with a human presence of technicians who can do the maintenance of the concrete blocks e.g. de-icing as well as sensors maintenance, iii) this station is located in a severe freezing environment area at 1,567 m of altitude, which was a pre-requisite for our experiments.

This station offers extreme meteorological conditions, such as frost thickness rate of 100 cm per 24h, absolute minimum temperature of -28°C (10 February 1956), absolute maximum temperature of +28°C (9 August 1923), maximum rate of variation of temperature up to 0.2°C/minute (12°C/h); the average number of days with snow fall is 66 per year and the number of days with snow cover of the ground is 120 per year. The maximum accumulated height of fresh snow in 24 hours is 1.86 meters (16 February 1976). It also fell 2.80 meters of snow in three days at the Aigoual in December 2002 and February 1996 was the snowest calendar month since the beginning of meteorological observations (1896) with a total of 4.50 meters.

In addition, the annual average number of frosty days is 144 with no day hotter than 25°C. The place is rather windy with 265 days per year of strong wind (> 16 m/s).

In terms of Köppen-Geiger climate classification [18], [19] these parameters of Mount Aigoual as well as Massif Central Puy de Dôme and French-Italian alpine region, (page 456 in [19]), correspond to cold continental / sub-arctic climate, coded by “Dfc”. As such, they can be compared to the classification of Nordic stations such as Boras (Sweden) classified as continental / humid coded “Dfb”, or Trondheim and Lillehammer (Norway) with a sub-arctic climate without wet season coded “Dfc’’ giving the evolution along the year of monthly averages, minimum (T_n) and maximum (T_x) temperatures and waterfalls for different relevant meteorological stations.

The graphical representation in **Figure 1** is called ombrothermic or climatic diagram. It clearly shows that temperature evolution along the year at Mount Aigoual is very similar to those of Boras and Trondheim, only Lillehammer having cooler temperatures **(Figure 1).**

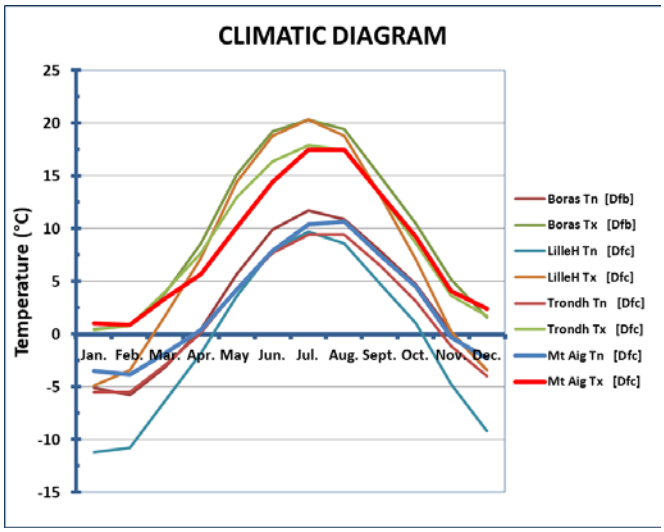

Figure 1: Climatic diagram comparing Mount Aigoual stations with relevant Nordic stations

A more precise assessment, taking into account all daily temperature measurements, can be given by comparing the distribution of temperatures measured at Mount Aigoual with Alpine ski resorts such as Courchevel or Alpe d'Huez, considered as among the coldest locations in France, as well as the French Massif Central (Town of Aurillac, Cantal district), Jura Mountain (town of Mouthe), a part of the Vosges and the Pyrénées Mountains.

When considering the histograms of minimum temperatures (T_n) of the two alpine ski resort stations cited above, Courchevel (1,850 m) and Alpe d'Huez (1,860 m) compared to Mount Aigoual **(Figure 2)**, the temperature distributions are very similar with quite the same statistical parameters: distribution range of 20°C (from 21 to 23°C) with similar extreme values (Tn between -11 and -14°C and Tx between °8 to +12°C) and a calculated mode of distribution centered on 1°C (Alpe d'Huez) or 3°C (Mount Aigoual and Courchevel) showing the representativeness of Mount Aigoual station with regards to the mountain climate met in the French alpine massif.

The standard deviation of the distribution is precisely the same with a value of 5°C, meaning most of the fluctuations occur in the range of temperature of [+5/-5°C].

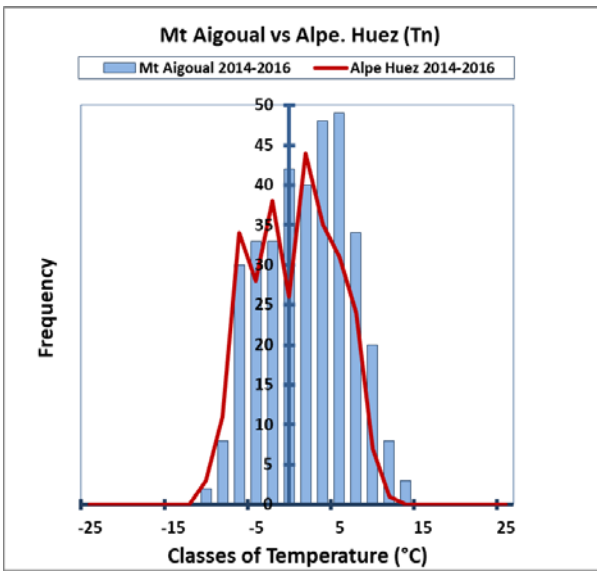

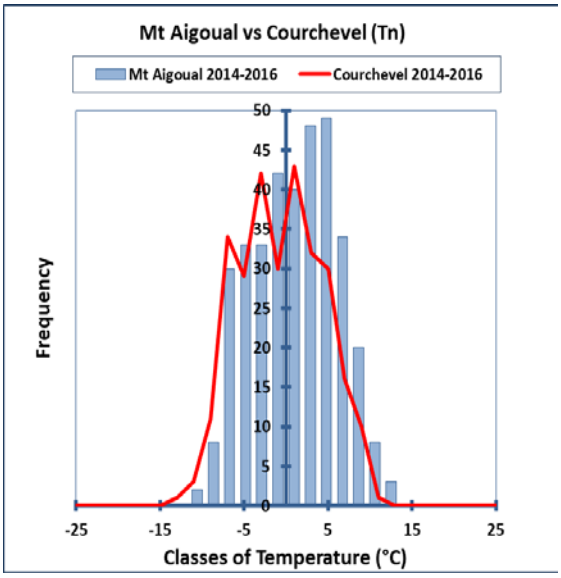

Figure 2: Distribution of minimum temperature (T_n) for Mount Aigoual compared to Alpe d'Huez (left) and Courchevel (right) met during winter periods from October 2014 to March 2016.

All the above characteristics demonstrate that the climate at Mount Aigoual is representative of a mountain climate which can be met in the French Alps, as well as in most of the Nordic countries, which is the first important result of this study.

2.2 Technical means

Sensors and records

The meteorological test centre is equipped with a test platform adequate for the deposal of the concrete blocks and equipped with different sensor types:

- **Screened temperature (°C):** probe Pt100. As it is located in a Stevenson shelter with double shelf in opposite orientation, this sensor is providing the air mass temperature without influence of wind and direct sun. This temperature is the reference parameter in meteorological studies.
- **Relative humidity (%):** Vaisala type HMP110 capacitive probe with operation range between 0 to 100% RH from -40°C to °80°C with precision data of ±4% within the temperature range -40 to 0°C and ±2.5 within the range of temperature 0°C to +40°C. It is also placed in the Stevenson shelter.
- **Direct temperature (°C):** Pt100 probe. As it is located on the test platform without protection, this probe is giving the temperature directly influenced by the sun effect.
- **Solar radiation (W/m^2):** pyranometer CMP6 from Kipp&Zonen. This probe is giving the sum of direct plus diffuse radiance. Solar radiation is one of the most important factors influencing the temperature distribution on Earth's surface, especially on massive concrete constructions. Average solar radiation arriving at the top of the Earth's atmosphere is roughly 1,361 W/m^2. When 1,361 W/m^2 is arriving above the atmosphere (when the sun is at the zenith in a cloudless sky), direct sun is about 1,050 W/m^2, and solar radiation on a horizontal surface at ground level is about 1,120 W/m^2. Obviously, the measured values at ground level will be influenced by the level of cloud cover that will shield the radiation flow reaching the Earth's surface.
- **Wind direction and intensity (m/s)** are registered with THIES ultrasonic heated type sensors.

Each of these sensors, related to the centralized multichannel datalogger of the Meteo-Station are giving values measured with a 6-minute interval, providing, per parameter, 240 values per 24h which means 7200 values for a 30-day month and 7440 values for a 31 day month).

Concrete samples

The two concrete blocks were cast in marine plywood formworks of dimensions: Length L = 60 cm, height h= 46 cm and thickness e = 17cm. Each block was equipped with 5 thermocouples, 4 located at 2 cm below the vertical faces and 1 located at the centre according to the sketch shown in **Figure 3**.

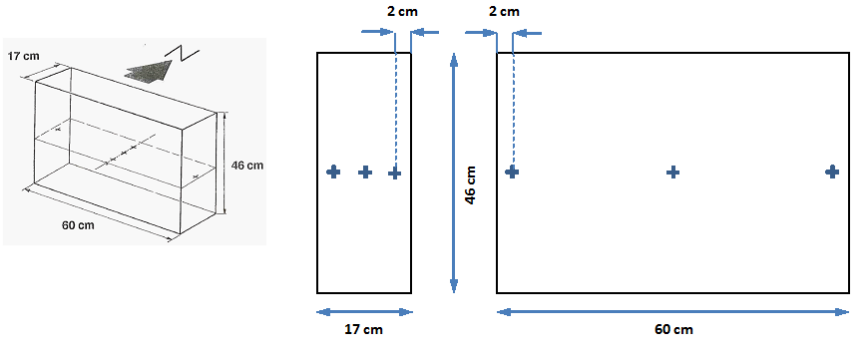

Figure 3: Schematic drawing of the concrete block and thermocouple positioning.

All the thermocouples feed a multichannel Squirrel data logger Grant type 2020 with numerical values with a 6- minute interval. The data logger is placed in a measuring cabinet kept frost-free by mean of heating resistors.
It must be pointed out here one important interest of the campaign which is all data (concrete temperature and meteorological parameters) are acquired with the same time interval.

Two concrete mix designs were used to cast the blocks, one corresponding to a XF4 mix design with air entrained and one corresponding to an Ultra High Performance Fiber reinforced concrete (UHPFRC). We report in this paper the results for the traditional XF4 concrete, whose mix design is given in **Table 1**.

	Type	kg/m3	Ratios	
Sand	0/4	600	S/G	0,39
Gravel 1	4/15	900	C/S	0,58
Gravel 2	15/20	650	E/C	0,45
		2150		
Cement	CEM I 52.5N	350		
Water		158		
Fluidizer	RheoBuilt 5000	5,25	(1,5% of cement weight)	
AEA	Air Bubble	14	(4% of cement weight)	

Table 1: XF4 concrete mix design

The blocks were placed without any thermal insulation, meaning that the frost attack was by all sides of the blocks. This configuration was chosen to measure the intrinsic response of concrete to the frost environment and not to simulate the behaviour of a sample prepared according to CEN/TS12390-9. This last configuration will be the topic of a forthcoming paper.

For the study of the concrete temperature (without de-icing salts), the blocks were placed upright (the height being vertical and the length being horizontal), the major faces oriented North-South as shown in **Figure 3**.

2.3 Thermal cycle and freeze-thaw parameters

In general terms, a thermal cycle is a fluctuation of temperature around a mean value between two extreme values. The extreme values are reached periodically with time. The simplest cycle is given by a sinusoid curve, which implies symmetry between the extreme values. The parameters attached to a cycle are i) full amplitude (peak to peak), ii) mean value understood as

the half of the full amplitude (peak to zero), iii) wavelength, and iv) increasing and decreasing rates.

Several definitions of freeze-thaw cycle can be found in the literature for climate considerations. For Baker and Ruschy [20], a FT cycle is a fluctuation of temperature around zero degree Celsius, fixing minimum daily temperature equal or lower than -3.5°C and maximum daily temperature equal or higher that +6.5°C. In 2006, Ho et al. in [21] reset the values as strictly higher that 0°C for daily maximum temperature and strictly lower than -1°C for daily minimum temperature. In 2005, Bourque et al. considered full amplitude of 8°C [+4/-4°C] [22].

Applied to conventional freeze- thaw cycles from the different test methods, these parameters become: i) full amplitude: 40°C, ii) mean value = 0°C, iii) wavelength: 12 or 24h and iv) freezing rate: between 2 and 10°C/h, depending on the test method. In other words, a periodic thermal cycle is passing through the mean value (0°C) twice per cycle, once per direction e.g. decreasing and increasing. In addition to these parameters, the duration at minimum temperature has to be taken into account with regards to degradation intensity. Freezing rates and duration at minimum temperature are closely linked together due the fact that, for a constant periodicity, if freezing rate increases, duration at minimum temperature also increases. If the impact on the degradation of concrete has been documented by Studer and Lindmark ([12] and [13]), these parameters remain in practice very variable from one climatic chamber to another and from one laboratory to another in the testing procedure, inducing scattering of the test results.

In the following section, we shall analyse thermal profile measurements with regards to thermal profile characteristics of the reference test method (Slab test) in CEN/TR 12390-9.

2.4 Numerical thermal modeling of concrete blocks temperature under real climatic conditions

In order to verify the dependence of the temperature profile in concrete with the solar radiation, the air mass temperature and other climatic processes, numerical modeling of the thermal behaviour of concrete blocks exposed to real climatic conditions was formulated. This was done with finite element software Cast3m using an implicit transient scheme “θ-method”, a method that allows solving a first-order differential equation obtained by spatially discretizing the heat equations on a finite element mesh. The model is non-linear to take into account the radiation effect.

It is important to note that, in reality, the heat transport mechanisms in porous materials such as concrete are complex. It can involve phase changes processes (vaporization, condensation and solidification due to freeze/thaw cycles and according to the material saturation state), thermal radiation between particles, and convective exchange in the porosity as well [23]. Since the porous media is relatively small compared with the volume of the solid matrix, we can neglect this process and reduce these complexities in a first step. The conductivity term is determined by the heat transferred between particles inside concrete material.

Problem formulation:

The applied boundary conditions on an exposed concrete block are the following:

- Convective exchange with air outside the boundary layer, i.e. outside the area where the air temperature is influenced by convective exchanges with the material.
- Solar radiation effect which is applied as a time-varying heat flux on the faces of the body, reduced to south face only.
- Thermal irradiation which corresponds to a thermal exchange between concrete and an environment located at infinity.

Each of these thermal exchanges will be described in details in the following parts.

In transient regime, the heat transfer is governed by the following general equation where the temperature T (°C) is defined at any point in space and at any time t(s) by Fourier's equation:

$$\Delta T = \frac{1}{a}\frac{\partial T}{\partial t}\,; \qquad (1)$$

where:

- Δ represents the laplacian operator, a, the diffusivity of concrete defined as $a = \frac{\lambda}{\rho.C}$
- λ is the concrete thermal conductivity, ρ, the density and C, the heat capacity of the material. The values of these parameters depend on the mix design formulation of concrete (water to cement ratio, percentage of entrained air, aggregate types, porosity …).

  Table 2 gives the approximated values of these thermal properties that are used in our model.

Material	**λ(W.K^{-1}.m^{-1})**	**c(kJ/kg/°C)**	**ρ (kg/m^3)**
Concrete	**1.5 (1.5-3.5)**	**0.84 (0.84-1.17)**	**2200 (2200-2400)**

Table 2: Thermal parameters of concrete blocks.

The values within the brackets are a range of the thermal properties of concrete. These parameters were studied in many researches such as Morabito and Quin and Hiller in [24], [25]**.** In the absence of any measurement of these thermal properties, the approximation of the used values was based on the mix design: since it is an air-entrained concrete, therefore it has a a thermal insulating capacity. A parametric study was carried out to study the effect of the choice of these properties, the model showed a stability and an insignificant dependency on the values of the thermal properties attributed to the concrete block. According to these boundary conditions, the following equations are selected to solve the problem.

Thermal convective flux

The thermal convective flux is given by the Newton's equation:

$$\varphi_{conv} = h\,(T_s - T_{air})\,; \qquad (2)$$

where φ_{conv} (W.m^{-2}) represents the convective flux between the surface and the air at a temperature T_{air}, T_s the surface temperature and h the convection coefficient depending on the air velocity and kinematic viscosity. Many correlations existing in the literature are used by

other researchers giving the evolution of h in function of wind velocities. These equations are all based on empirical models verified on observations and experimental comparisons. In this study, we used the following equation given by Smith in [26]:

$$h = 6.22 + 8.73 \times V^{0.652} \quad (3)$$

where V is the wind velocity (m/s) measured and reported by weather stations. Since we assumed that the majority of the concrete thermal behaviour is due to the interaction with the air mass and direct temperature (this last one being a consequence of the solar radiation), we injected air mass temperature (screened temperature) and solar radiance flux as inputs of the thermal model. **Figure 4** is giving an example of the fluctuations of these measured parameters in function of time.

Solar radiation flux

Solar radiation presents the sum of two components: direct flux and diffuse flux components. The latter comes from the deviation of part of the direct solar radiation during its passage through the atmosphere by optical phenomena, and in particular from the effects of reflection and refraction by water droplets present in the atmosphere and in clouds.

Solar radiation propagates energy as short waves arriving on the materials surface. In this study, we did not calculate the value of solar flux since we have the data from the meteorological station of the solar radiance (W/m^2) measured by a pyranometer for the whole period of study.

The material absorbs this energy according to its value of absorptivity γ_{abs} which depends on the surface color and range from 0.5 to 0.9 for new and older concrete, respectively. In this study $\gamma_{abs} = 0.8$ used in [25].

Thermal long- wave radiation heat flux

The thermal long-wave radiation heat flux φ_{irr} corresponds to the radiation between the concrete surface and the sky and can be calculated by the following equation:

$$\varphi_{irr} = \varepsilon \times \sigma(T_s^4 - T_{sky}^4); \quad (4)$$

Where ε represents the concrete material emissivity which is approximated to 0.90, σ the Stephan-Boltzmann coefficient equal to 5.67×10^{-8} ($W.m^{-2}.K^{-4}$) and T_{sky} the effective sky temperature which is different than the air temperature (it is actually the temperature of a blackbody radiation having the same flux as the downward atmospheric radiation and is not equal to air temperature [25]). Concerning the determination method of this variable, a portable infrared thermometer can quickly measure the sky temperature; however, this instrument cannot give an accurate measurements as required [27]. Researchers from other domains have designed and constructed prototype devices in the laboratory to measure the sky temperature; however, no such a device has been universally proven to give accurate measurements. Instead, the down welling long wave radiation can be more precisely measured by a pyrogeometer or radiometer. However, due to the high cost of equipment and the challenge of instrument calibration and quality control, the measurement of long wave radiation is still rarely available [27]. Many correlations exist to estimate the value T_{sky}. In the absence of dew point temperature data (T_{dp}), T_{sky} can be assumed as 6 K below the ambient dry bulb air temperature [28], and

cited in [23] and [29]. Despite the fact that $T_{air} \neq T_{sky}$, many researchers have used T_{air} in the Stephan-Boltzmann relation **(5)**. More precisely, the sky temperature is much lower than the ambient air temperature [30]. In our study, we used the following relation given by Berdhal and Fromberg in [31]:

$$T_{sky} = \varepsilon_{sky}^{0.25} \times T_{air}; \quad (5)$$

where ε_{sky} is the sky emissivity given in clear weather as follow [32]:

$$\varepsilon_{sky} = 0.754 + 0.0044 \times T_{dp}\ ; \quad (6)$$

Since we didn't have access to the whole meteorological data measurements of the dew point temperature, T_{dp} was estimated by the equation used by [33]:

$$T_{dp} = \frac{243.04 \times \alpha(T,RH)}{17.625 - \alpha(T,RH)}\ ; \quad (7)$$

$$\alpha(T,RH) = \ln\left(\frac{RH}{100}\right) + \frac{17.625 \times T}{243.04+T}; \quad (8)$$

where RH is the relative humidity in (%), this correlation is given for T ranging between -40°C and +50°C.

3. Results and discussion

3.1 Concrete temperature profiles and meteorological parameters

The time series of XF4 concrete temperatures (°C), in combination with the screened (air mass) temperature (°C) and the solar radiance, raw and moving average (Y' axis in W/m^2), the Y axis being normalized to the thermal cycle of CEN/TS 12390-9, are reported in **Figures 4** and **5**.

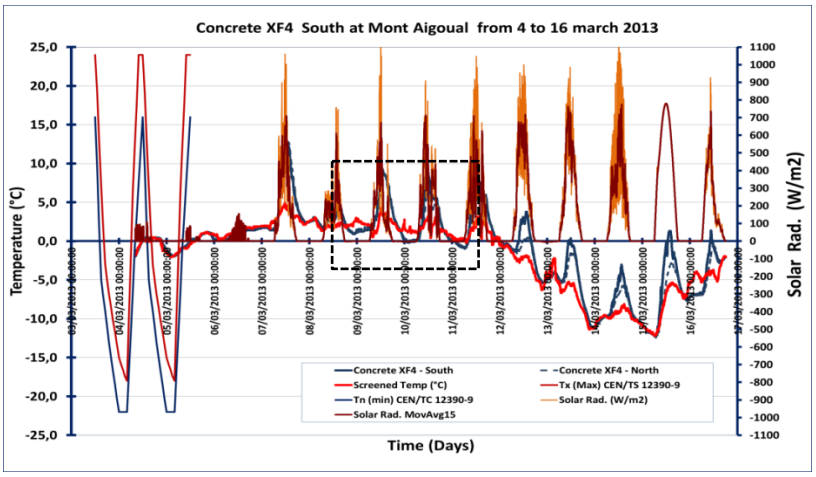

Figure 4: Time series of internal temperature of concrete in blue, screened temperature in red (Y axis) and solar radiance in orange with moving average in brown (Y' axis) with reference to CEN/TS 12390-9 thermal cycle (Tx in red, Tn in blue).

At the time scale of the figure (over 10 days), we can make several observations:

i) The general shape of the concrete temperature curves can be interpreted in terms of signal analysis. With intensity variations strongly correlated to solar radiance and screened temperature, we can describe the concrete temperature signal as the sum of a “bearing curve” characterized by low frequency and low intensity variations, on which are superimposed high frequency and high intensity fluctuations. Being correlated to the screened temperature, this bearing curve represents the regional contribution of the air mass to the concrete temperature with, in addition, high frequency fluctuations strongly correlated to the solar radiance indicating that they are related to the effect of the direct sun to the concrete surface. The periodicity of 24h of the thermal signal is strongly induced by night-day alternation and fluctuations of solar radiation.

ii) The strong asymmetry of the temperature curves appears to be not consistent with the very regular and symmetric temperature profile imposed in the different test methods for assessing scaling. However, the strong asymmetry of the measured temperature in concrete is consistent with rock temperature measurements at few centimetres deep inside the rock face, reported in climatology studies of alpine regions dedicated to rocky risk,[34]–[37]. The strong asymmetry of the temperature profile is subsequently a characteristic of thermal behaviour of concrete under local climate and exposure, as well as rock faces in severe cold environment.

iii) The fluctuations of the concrete temperatures are strongly correlated to those of the solar radiance and to a lesser extent, to the screened temperature (air mass temperature). This means obviously that the day/night alternation is governing the solar radiance alternation and during daylight period, direct sunshine is responsible for the temperature increase compared to air mass values, as well as fluctuations. During daytime, when the solar radiance is strongly reduced by shadowing effect due to a cloud cover, its value can be lowered from 1 110 W/m^2 (maximum value) to less than 200, eventually down to zero. In such conditions, concrete temperatures are clearly reduced (superimposed) to the bearing curve, corresponding to the air mass temperature. This situation is particularly visible in **Figure 4** from the 7th to the 16th of March at the left end side of the time series and for each night-time.

iv) Considering one single record (XF4 South for example), the temperature as a “signal” is strongly asymmetric in contradiction to the thermal cycle from the CEN/TS 12390-9. This asymmetry is characterized by an expansion towards positive values compared to screened temperature during daytimes and almost a flat profile during nighttimes. This led us to differentiate between cooling and freezing rates with the first one being far higher than the second, as a rule of thumb. It is also noticeable to observe the fast convergence of concrete and screened temperature curves, which may become fully super imposable or very close together. This would imply that under these conditions, concrete reaches the thermodynamic equilibrium relatively fast. These observations are consistent with previous measurements made in Centre of Snow Study (1992).

v) This observation is also valid during all night times. A precise observation shows that if there is a strong time correlation between solar radiance and screened temperature, there is a slight time lag between the maximum of solar radiance peak and the maximum temperature peak. This time lag is varying between 30 to 90 minutes (**Figure 5**).

vi) Each individual temperature curve (corresponding to each geographic orientation) is quite super imposable to each other with some differences in intensities due to differential impact of solar radiation on each face, and showing a time lag between sensors limited to a maximum of 1.5 hrs between [South-West-East] and [North-Centre] faces. (**Figures 4** and **5**).

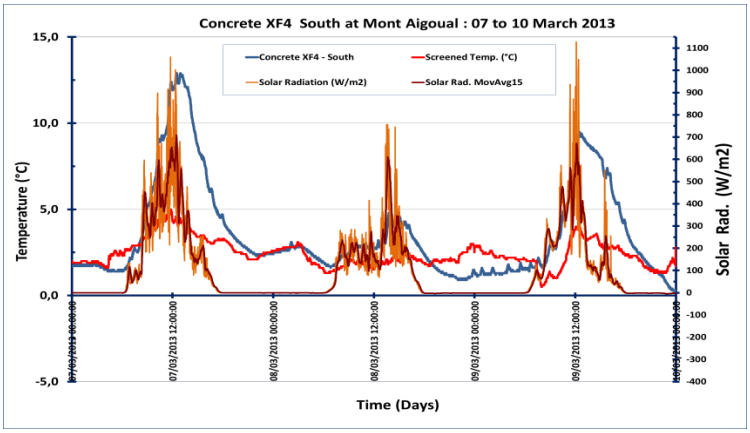

Figure 5: Time series of concrete and screened temperature and solar radiance over a period of 3 days showing detailed variations and relationship between these parameters.

3.2 Thermal modeling results

Figures 6 and **7** show the results of the simulation compared with experimental measurements both at 2 cm from XF4 concrete block-south face for two different periods of time:

- From the 4th to the 15th of March 2013.
- From the 16th of February to the 2nd of March 2015

As a result, a simplified numerical model can correctly simulate the behaviour of concrete exposed to temperature variations and subjected to convective and radiative heat exchanges, only by taking as input the variations of screened temperature and the solar radiance evolution in function of time.

A slight shift is observed between numerical results and experimental measurements that can be explained by the faster temperature distribution and propagation inside the material in the simulation than in the real case.

However, modeling the thermal behaviour of concrete by taking only into account the variations of screened temperature and the solar radiance evolution as a function of time as input isn't sufficient.

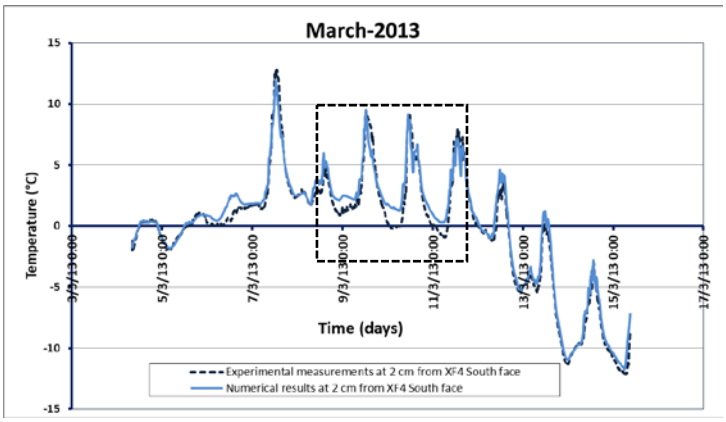

Figures 6: Concrete temperature measurements versus numerical results from 4th to 15th of March 2013 at 2 cm from XF4-South face.

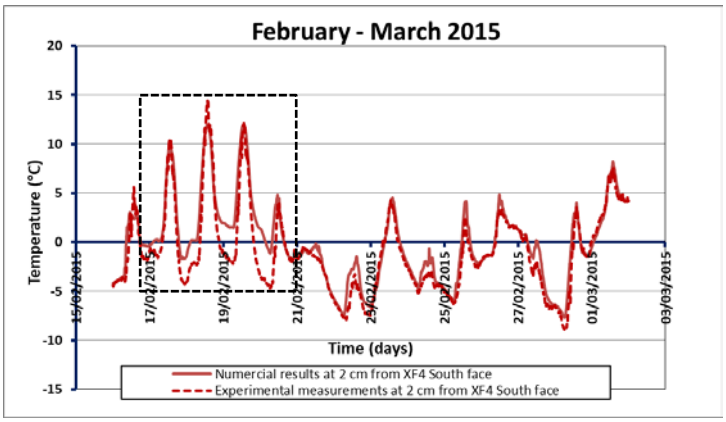

Figures 7: Concrete temperature measurements versus numerical results from 16th of February to the 2nd of March 2015 at 2 cm from XF4-South face.

The numerical model doesn't fit the experimental results in some specific periods squared in **Figures 6** and **7.** This is especially the case of negative temperature peaks that concrete undergoes at night period, while no particular problem was observed for positive temperature. Concrete has a more complex reaction in natural environment, which has to be taken into account in the model. Data from the meteorological station indicate that the visibility was high during these specific nocturnal periods, wind velocities were less than 3 m/s as well, relating those phenomenon to nocturnal radiation process [30], [38]. In meteorology, visibility is a measure of the distance at which an object or light can be clearly discerned. Low visibility is generally caused by low lying stratus clouds, air pollution, heavy rains, high humidity and fog as well. At night, especially in clear weather and in case of small wind velocity, the drop in temperature is caused by a cooling of the concrete, the latter transmitting its fresh temperature to the air just above. The temperature drop is also noticeable (the concrete can be much colder at night than the air temperature and we may find concrete surface with a temperature below 0°C even if it is 1, 2 or 4°C at 1m above the block). This can be seen in **Figure 4** (in the squared period), where concrete is colder than the surrounding air. Thus, the moisture (dew) that settles freezes and white frost can appear even if the temperature at 1m above the concrete is positive. The white frost is formed when the wind velocity is relatively small or negligible, which is our case. White frost is not related to the super cooling phenomenon, unlike ice. It is immediately triggered as soon as the air containing the water vapour near the solid surface cools by solid condensation (change from a gaseous to a solid state).

In order to integrate this process inside the model, the effect of thermal long-wave radiation heat flux φ_{irr} during the periods where nocturnal radiation occurs was amplified, by using the Lienhard previously cited correlation [28] and cited in [23] and [29], according to the following equation:

$$T_{sky} = T_a - c \qquad (9)$$

where c is a constant ranging from 0 to 20. This correlation was used in [28] with c = 6 K. Without meteorological data concerning the cloud coverage affecting the nocturnal radiation process, the above correlation was used. Furthermore, it allows enhancing the effect of the thermal long-wave radiation heat flux at the same time. Results are shown in **Figures 8** and **9.**

The improvement of the numerical model is clearly visible by amplifying the thermal long-wave radiation flux effect during night (nocturnal radiation) during specific time periods defined as periods of high visibility and slow wind velocity. Numerical results became closer to experimental measurements in nocturnal periods. The numerical simulations are without taking into account the formation of white frost that can be formed on the concrete surface due to nocturnal radiation at these periods as explained above.

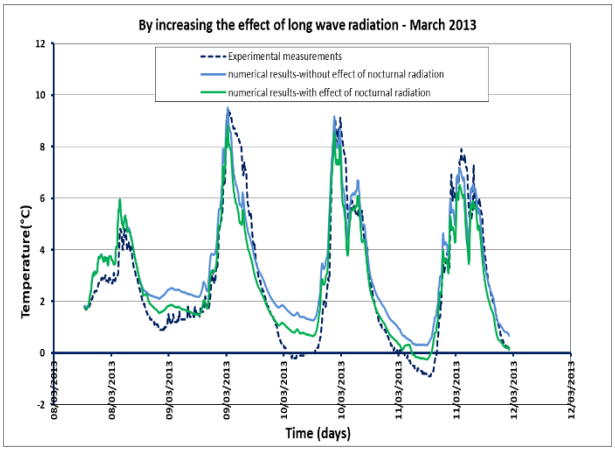

Figures 8: Comparison of numerical results to experimental measurements after taking into account nocturnal radiation-March 2013

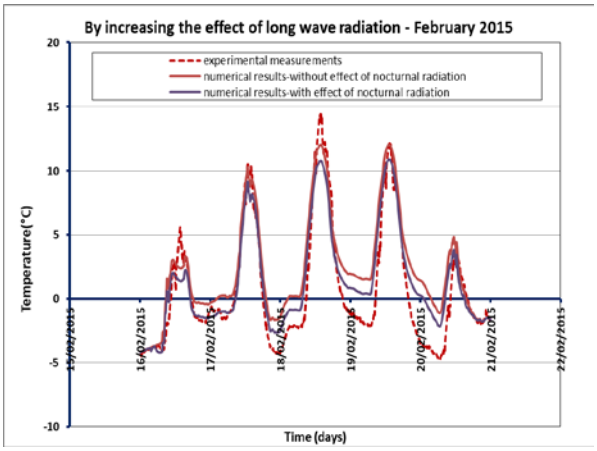

Figures 9: Comparison of numerical results to experimental measurements after taking into account nocturnal radiation-February 2015

However, it seems interesting to move to a more detailed modeling by integrating more meteorological parameters to have a complete model that can be used in all types of weather. Initial results show that simplified models could be used to describe concrete behaviour and evaluate temperature variations near the surface or in the body of the structure under study. A work is ongoing to couple this thermal model to a mechanical approach to express concrete damage under freeze and thaw actions including the effects of pore pressures: hydraulic by Powers **[1]**, osmotic by Powers and Helmuth [39], crystallization by Scherer [40], in order to have a complete model taking into account the maximum of processes that concrete undergoes under freeze/thaw degradation.

3.3 Analysis of freeze-thaw cycles

The statistical analysis was done over a period of three winter seasons (October to march) from 2013 to 2015. This corresponds to 54 time series of 10 days each, for which we determined the number of thermal cycles, freezing and thawing or not. A freeze-thaw cycle is defined as a temperature profile passing through the 0°C isotherm twice per 24h. For each cycle, the thermal amplitude has been characterized.

The result of this analysis, consistent with several other on- site measurements **[28, 29, 31, 35]** can be summarized in defining three type of thermal cycles occurring in winter environment: i) ≪thawing cycles≫ with a thermal amplitude of 15°C [+15°C/0°C], ii) ≪freeze-thaw cycles≫ with a thermal amplitude of 10°C [+5°C/-5°C] or [+2°C/-8°C] and iii) ≪freezing cycles≫ with a thermal amplitude of 7.5°C [0°C / -7.5°C].

The number of freeze-thaw cycles is around 5 per month, which is very low compared to the 30/31 cycles per month delivered by the laboratory test methods. On this basis, these results suggest that the laboratory conditions correspond to an acceleration rate by a factor 6.

In terms of cooling and freezing rates, the analysis leads to a cooling rate of 0.9°C/h (temperature drops from +6 to -1°C in 8h) and to a freezing rate of 0.7°C/h (temperature drops from -1 to -4 ±1°C). These findings e.g. most frequent Freeze-Thaw cycles between [+5°C/-5°C] and Freeze cycles between [0 or -2/-10°C] or [-3°C/-15°C] are very consistent to previous observations reported by Kaufmann [14], [37] and by Cusson, Qian and Hoogeven in [41].

Assuming an homogeneous cooling/freezing rate between +6°C to -5°C in 14h, this gives a mean freezing rate of 0.78°C/h much lower than the freezing rate of the slab test as the reference method in the CEN/TS (1.9°C/h), but closer to the freezing rate of the German cube, first alternative method, (1.5°C/h) and out of comparison with the CDF Test, second alternative method (10°C/h).

As a preliminary conclusion, FT cycles with full amplitude of 40°C and freezing rate higher than 1.5°C/h appear to be very rare in such common meteorological conditions. This is a second important finding of our study.

Based on the above considerations and as long as freezing rate is considered as a critical parameter governing the intensity of scaling [12], [13], [42], the representativeness of the test methods and their inter-comparison is still questionable.

3.4 Concrete and screened temperatures: Statistical distributions

Another noticeable observation can be made when comparing the distributions of measured values (histograms) at Mount Aigoual between air mass and internal (center) concrete temperature under same local meteorological conditions (wind velocity, cloud covering and relative humidity). (**Figure 10**) shows the great similarity of these two distributions during December 2014 and this same result was observed during all other studied periods of time.

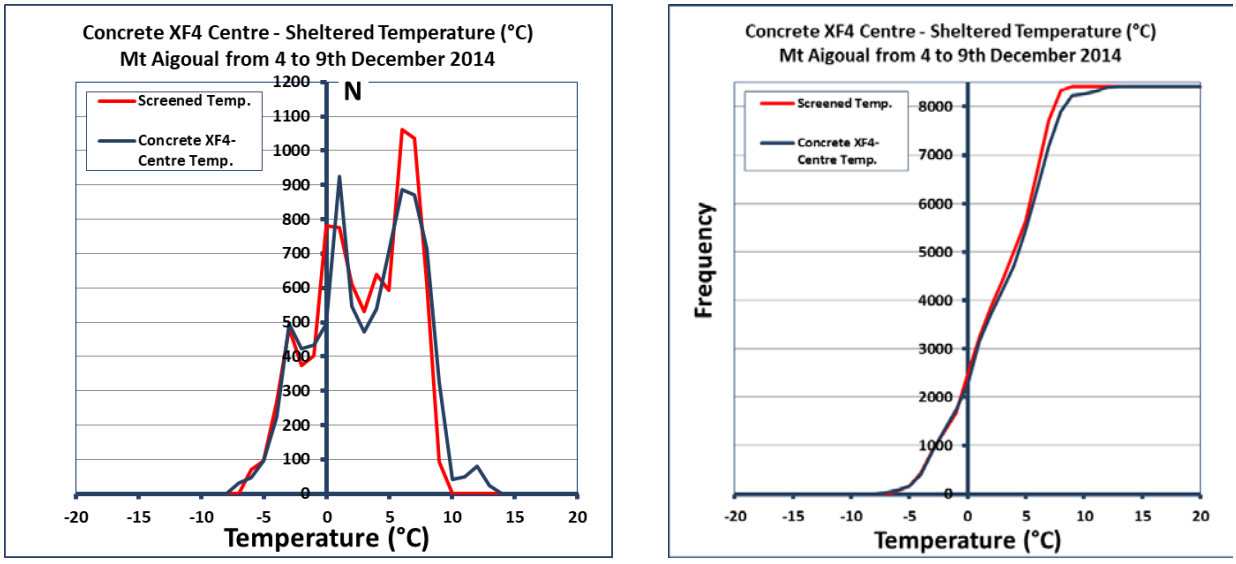

Figure 10: statistical and cumulative distributions of screened temperature and XF4 Centre concrete temperature,

showing highly similar temperature distributions-December 2014.

This result seems surprising but can be understood by taking into consideration that concrete is behaving like a Stevenson shelter, preserving the thermocouple from variations of parameters known to influence temperature measurements: intensity of light (solar radiation), wind velocity and relative humidity.

A practical consequence of this similarity of distributions is the ability to predict the internal concrete temperature (at 6 cm deep) by considering the screened (air mass) temperature of any site from its meteorological data available from national web sites. This is the third important finding of this study.

3.5 Comparison of Mount Aigoual with other European cold areas

Taking benefit from the conclusion above, temperature measurements were downloaded (daily or hourly averages) from national website of Norway, Sweden and Finland. From Norway the daily averages screened temperature (T_x and T_n) for a full winter season from October to February: Oslo 2013-2014 (**Figure 11**) and Trondheim 2014-2015 (**Figure 12**) were obtained.

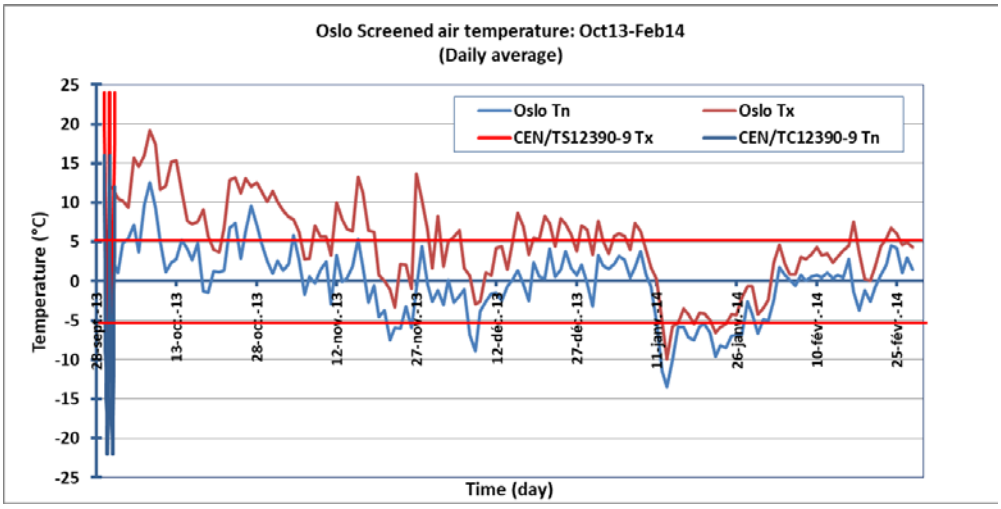

Figure 11: Time series of daily average screened temperature [Min (T_n); Max (T_x)] for Oslo Station with CEN/TS12390-9 thermal cycle as a reference at the same scale of time.

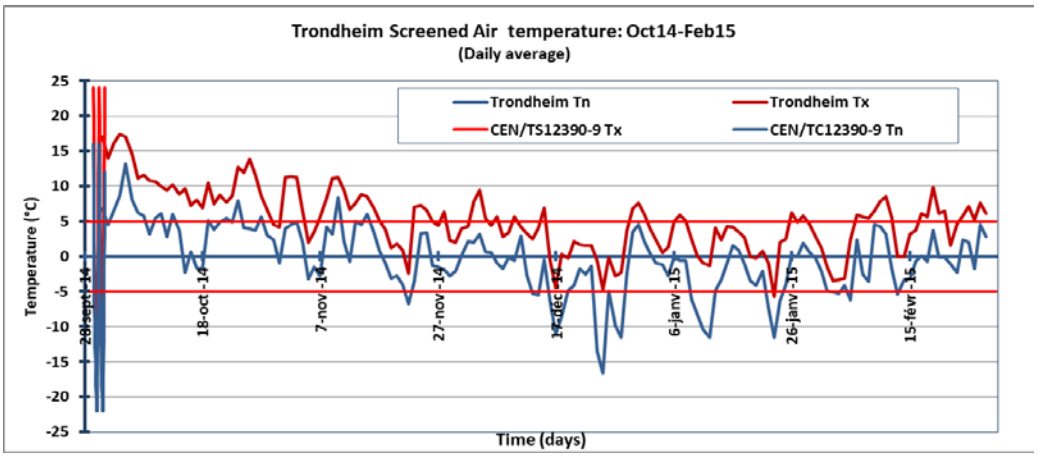

Figure 12: Time series of daily average screened temperature [Min (T_n), Max (T_x)] for Trondheim

Station with CEN/TS12390-9 thermal cycle as a reference at the same scale of time.

From the time series in **Figures 11** and **12** a full conventional freeze-thaw cycle amplitude of [+20/-20°C] never occurs. The maximum temperature of the thermal cycles is fluctuating between +10°C to +5°C, this last one being the most frequent, while the minimum temperature is fluctuating around -5/-10°C. When temperature is down to -10°C or -17°C, the maximum temperature is not higher than +2°C. Even if these examples do not correspond to an extensive statistical analysis, these observations confirm our data from Mount Aigoual.

In Sweden, hourly averages values from Borås station showed that when the temperature is regularly cycling, the full amplitude is 15°C, values ranging from [+5/-10°C] (**Figure 13**).

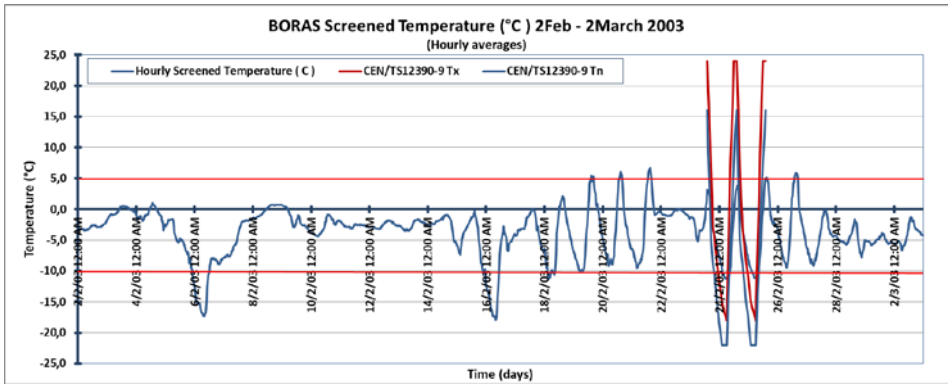

Figure 13: Time series of daily average screened temperature for Boras Station from Feb to 2 March 2003

Most of the freeze-thaw fluctuations have full amplitude of 15 °C, ranging from [+5/-10°C]. When the minimum temperature is reaching colder values e.g. -15°C, the maximal temperatures do not exceed 0°C corresponding to what we called “freezing cycle (**Figures 13**). These situations are also consistent with our measurements in Mount Aigoual.

These comparisons confirm again our finding from Mont Aigoual that F/T cycles with full amplitude of 40°C practically doesn’t exist, for the considered geographic location.

4. Conclusions

From Mount Aigoual meteorological station, representative of mountain and arctic climates, our measurements of internal temperatures of concrete placed in a severe winter environment are characterized by the following:

- In contradiction to most of conventional FT cycles used in practice for FT testing, the thermal profile of concrete is strongly asymmetric with a positive temperature branch more developed compared to the negative temperature branch. Corresponding cooling rates, ranging from +20°C/0°C are much higher than freezing rates ranging from 0°C/-10°C.
- The full amplitude of the thermal cycle has never been found equal to 40°C [+20/-20°C] but rather 15°C [+10/-5°C] or [+5/-10°C]. This range seems to be also representative of Nordic countries according to data from official meteo websites. The corresponding

freezing rates are ranging between 0.6 to 1.5°C/h, which is close to the German Cube test conditions and not far from Slab test conditions.

- The number of natural "true" freeze- thaw cycles (passing through 0°C isotherm twice per 24h) is five times less than the 24h based standardized tests.

All these reasons give a strong incentive for full characterization of the natural environment when correlations have to be made between laboratory test results and on-site degradation of concrete, both submitted to freezing and thawing conditions. The consequences of these data are threefold:

i) Reducing the full amplitude of FT cycle from 40°C to a more representative value e.g. 15°C to 20°C, should have an impact on working conditions of climatic chambers i.e. internal ventilation. This should affect positively reliability.

ii) The effect of freezing cycles (temperature cycling under negative temperatures) has to be taken into account considering freezing mechanisms in a porous media such as concrete, which is characterized by a wide pore size distribution and a pore solution chemical composition changing with age and dominated by Ca^{2+}, Na^{+}, K^{+}, HO^{-}, $SO4^{2-}$ and Cl^{-} ions.

iii) A full thermal amplitude of 15 to 20°C seems to be the most frequent temperature range e.g. [+10°C/-5 or -10 °C] for mild climate, [+5/-10 or -15 °C] for mountain climate in western and northern Europe and [-10/-25°C] for very severe environment in continental climate.

Acknowledgements

The authors address sincere thanks to Christian Clergue (Sigma Béton) for providing technical support in producing concrete blocks and the technical maintenance of the recording system. The authors also thank Fernand Deillon and Amélie Bazzoni from TFB (Switzerland) for the very fruitful discussions leading to the final version of this paper.

Thanks are also addressed to the Meteo-France team in Mount Aigoual (Chantal Vimpere and Christian Pialot) for their technical assistance and on- site maintenance as well as their constant warm welcomes in the premises of the meteo station in Mount Aigoual.

The financial support of this work by ATILH (Technical Association of French Cement Industry) and the grant by ANRT by mean of CIFRE convention n°2017/891 are great fully acknowledged.

References

[1] Powers, *The air requirement of frost resistant concrete*. 1949.

[2] C. Pigeon, M.; Gagné, R.; Foy, "Critical air void spacing factor for low water-cement ratio concretes with and without condensed silica fume.," *Cem. Concr. Res.*, vol. 17, no. 6, pp. 896–906, 1987.

[3] D. H. Bager, "Ice formation in room temperature cured mature hardened Portland," no. c, pp. 709–720, 1986.

[4] G. Fagerlund, "Frost resistance of high performance concrete," Lund, 1993.

[5] M. Pigeon, J. Marchand, and R. Pleau, "Frost resistant concrete," *Constr. Build. Mater.*, vol. 10, no. 5 SPEC. ISS., pp. 339–348, 1996, doi: 10.1016/0950-0618(95)00067-4.

[6] M. Marchand, J., Pigeon, "Résistance du béton à l'écaillage dû au gel en présence de sels fondants - Une revue des récents développements dans le domaine," in *Conférence RILEM : Béton - Du matériau à la*

structure, 1996, pp. 179–2010.

[7] T. Siebel, E., Reschke, “Three different methods for testing the freeze-thaw resistance of concrete with and without deicing salt - European round robin test,” in *Rilem proceedings 30 Freeze-Thaw Durability of Concrete*, 1997, pp. 231–246.

[8] M. J. Setzer and R. Auberg, “Freeze-thaw and deicing salt resistance of concrete testing by the CDF method CDF resistance limit and evaluation of precision,” *Mater. Struct.*, vol. 28, no. 1, pp. 16–31, 1995, doi: 10.1007/BF02473288.

[9] C. 12390-9 Document, “CEN/TS 12390-9, “Testing hardened concrete. Freeze-thaw resistance-Scaling“.,” 2017.

[10] M. Marchand, J., Sellevold, E.J., Pigeon, “The deicer salt scaling deterioration of concrete,” *An overview, ACI Spec. Publ. SP-145*, pp. 1–46, 1994.

[11] M. Marchand, J., Pleau, R., Pigeon, “Precision of tests for assessment of the deicer salt scaling resistance of concrete,” *Cem. Concr. Aggregates*, vol. 18, no. 2, pp. 85–91, 1996.

[12] W. Studer, “Internal comparative tests on frost deicing salt resistance,” Canada, 1993.

[13] S. . Lindmark, “Mechanisms of salt frost scaling of Portland cement-bound materials : Studies and hypothesis, Thèse de doctorat,” Lund Institute of Technology, Sweden, 1998.

[14] J. P. Kaufmann, “Experimental identification of ice formation in small concrete pores,” *Cem. Concr. Res.*, vol. 34, no. 8, pp. 1421–1427, 2004, doi: 10.1016/j.cemconres.2004.01.022.

[15] A. M. Kjeldsen and M. R. Geiker, “On the interpretation of low temperature calorimetry data,” *Mater. Struct. Constr.*, vol. 41, no. 1, pp. 213–224, 2008, doi: 10.1617/s11527-007-9239-8.

[16] “BRITE Project Report,” 1992.

[17] L. Izoret, “Mécanismes de dégradation du béton soumis au gel en présence, ou non, de sels de déverglaçage.,” in *Durabilité du béton soumis au gel. ANNALES DE L’ITBTP*, 1991, pp. 75–87.

[18] W. Köppen, “Das geographisca System der Klimate,” in *Handbuch der Klimatologie*, 1936, pp. 1–44.

[19] M. T. A. Peel, M.C., B. L. Finlayson,B.L., “Updated world map of the Köppen-Geiger climate classification,” *Hydrol. Earth Syst. Sci. Discuss. Eur. Geosci. Union*, vol. 4, no. 2, pp. 439–473, 2007.

[20] D. L. Baker, D. G., and Ruschy, “Calculated and measured air and soil freeze-thaw frequencies,” *J. Appl. Meteorol.*, vol. 34, pp. 2197–2205, 1995.

[21] E. Ho and W. A. Gough, “Freeze thaw cycles in Toronto, Canada in a changing climate,” *Theor. Appl. Climatol.*, vol. 83, no. 1–4, pp. 203–210, 2006, doi: 10.1007/s00704-005-0167-7.

[22] F.-R. Bourque, C. P. -A., Cox, R. M., Allen, D. J., Arp, P. A., and Meng, “Spatial extent of winter thaw events in eastern North America: historical weather records in relation to yellow birch decline.,” *Glob. Chang. Biol.*, vol. 11, no. 9, pp. 1477–1492, 2005.

[23] M. Hall, P. Dehdezi, A. Dawson, and J. Grenfell, “Influence of the thermo-physical properties of pavement materials on the evolution of temperature depth profiles in different cliamtic regions.,” *Hall al*, 2010.

[24] Morabito P., “Thermal properties of concrete variation with temperature and during the hydration phase Department of Civil & Mining Engineering &Division of Structural Engineering: Milan, Italy; 2001.,” Milan, Italy, 2001.

[25] Y. Qin and J. E. Hiller, “Modeling temperature distribution in rigid pavement slabs: Impact of air

temperature," *Constr. Build. Mater.*, vol. 25, no. 9, pp. 3753–3761, 2011, doi: 10.1016/j.conbuildmat.2011.04.015.

[26] J. O. Smith, "Determination of the convective heat transfer coefficients from the surfaces of buildings within urban street canyons," University of Bath, 2010.

[27] K. Zhang, T. P. Mcdowell, and M. Kummert, "Sky Temperature Estimation and Measurement for Longwave Radiation Calculation Polytechnique Montréal , Dept . of Mechanical Engineering , Montréal , QC , Canada Thermal Energy System Specialists , LLC , Madison , WI , USA Abstract Modelling longwave heat ," no. 3, pp. 2093–2102, 2017.

[28] J. H. Lienhard IV and J. H. Lienhard V, *A HEAT TRANSFER TEXTBOOK, fourth edition*, Fourth Edi. Cambridge: PHLOGISTON PRESS, 2017.

[29] N. Le Touz, "Conception et étude d'infrastructures de transports à énergie positive : de la modélisation thermomécanique à l'optimisation de tels systèmes énergétiques," Ecole Centrale de Nantes, 2018.

[30] B. Bokor, L. Kajtár, and D. Eryener, "Nocturnal Radiation: New Opportunity in Building Cooling," *Energy Procedia*, vol. 112, no. October 2016, pp. 118–125, 2017, doi: 10.1016/j.egypro.2017.03.1072.

[31] P. Berdhal and R. Fromberg, "an Empirical Method for Estimating the Thermal Radiance of Clear Skies," *Sol. Energy*, 2012.

[32] R. Tang, Y. Etzion, and I. A. Meir, "Estimates of clear night sky emissivity in the Negev," vol. 45, pp. 1831–1843, 2004, doi: 10.1016/j.enconman.2003.09.033.

[33] M. G. Lawrence, "The relationship between relative humidity and the dewpoint temperature in moist air: A simple conversion and applications," *Bull. Am. Meteorol. Soc.*, vol. 86, no. 2, pp. 225–233, 2005, doi: 10.1175/BAMS-86-2-225.

[34] C. Chaix, "Winter climatology of alpine districts. PhD (in French)," Université de Savoie. Chambery, France, 2007.

[35] T. Morin, "Follow up of seasonal frost in the French Alps. MSc (in French)," 2013.

[36] Y. Feuillet, "Periglacial forms in French pyrennees: spatial and chronological analysis and valuation. PhD (in French)," University of Nantes, France, 2010.

[37] J. P. Kaufmann, "Experimental identification of damage mechanisms in cementitious porous material on phase transition of pore solution under frost deicing salt attack" - Thesis n°2037," EPF Lausanne, Switzerland, 1999.

[38] D. S. Parker, J. R. Sherwin, and A. H. Hermelink, "NightCool : A Nocturnal Radiation Cooling Concept Description of the NightCool Concept," *ACEEE Summer Study Energy Effic. Build.*, pp. 209–222, 2008.

[39] T. C. Powers and R. A. Helmut, "Theory of Volume Changes in Hardened Portland Cement Paste During Freezing," *Proc. Highw. Res. Board*, vol. 32, pp. 285–297, 1953.

[40] G. W. Scherer, "Stress from crystallization of salt," *Cem. Concr. Res.*, vol. 34, no. 9, pp. 1613–1624, 2004, doi: 10.1016/j.cemconres.2003.12.034.

[41] T. Cusson, D., Qian, S Hoogevenn, "Field performance of concrete repair systems on highway bridge," *ACI Mater. J.*, vol. 103, no. 5, pp. 366–373, 2006.

[42] M. H. Tremblay, "Scaling of concrete containing supplementary cementing materials: influence of maturation methods used on job sites site on scaling behaviour in laboratory chipping," Quebec, Canada, 2009.